Sliding Mode Control Algorithms for Wheel Slip Control of Road Vehicles

Conference Paper · July 2017

DOI: 10.23919/ACC.2017.7963616

4 authors:

Gian Paolo Incremona
Politecnico di Milano
60 PUBLICATIONS **981** CITATIONS
SEE PROFILE

Enrico Regolin
University of Pavia
17 PUBLICATIONS **132** CITATIONS
SEE PROFILE

Alessio Mosca
University of Pavia
3 PUBLICATIONS **15** CITATIONS
SEE PROFILE

Antonella Ferrara
University of Pavia
402 PUBLICATIONS **8,355** CITATIONS
SEE PROFILE

Sliding Mode Control Algorithms for Wheel Slip Control of Road Vehicles

Gian Paolo Incremona, Enrico Regolin, Alessio Mosca and Antonella Ferrara

***Abstract*— Sliding mode control approaches are presented in this paper for the wheel slip control of road vehicles. The major design requirement for the controllers is to make the wheel slip ratio follow a desired value, while guaranteeing that the sliding mode control is stabilizing. Its robustness in front of matched and unmatched uncertainties and data transmission delays is assessed in simulation. In the present paper different algorithms of first and second order type and integral or non integral nature are discussed. Simulation results are reported and analyzed, putting into evidence the superior performance, in the considered automotive context, of the integral sliding mode control.**

I. Introduction

The problem of controlling the longitudinal dynamics in road vehicles has been studied in depth in the past few decades. Control theory has been widely used to pursue the objective of maximum tire-road adherence during acceleration phases, i.e., Traction Control (TC), and braking phases with the so-called Anti-Lock Brake System (ABS). With the new available technologies, like multi-actuated vehicles with electric motors for each wheel, it is now possible to merge the problems of TC and ABS control in a unique Fastest Acceleration/Deceleration Control (FADC) problem [1]. In all critical situations, where maximum tire/road adherence is needed, the designed controller should track a target slip-ratio, selected on the base of suitable tire friction models [2], [3].

The implementation of a feedback control requires several quantities to be known (vehicle velocity, wheel-slip, tire-road friction coefficient), so that the states of the adopted model can be estimated. The problem of estimation of these values has been studied in recent years, also by means of sliding mode observers [4]–[7]. Sliding Mode Control (SMC) theory has been a popular choice for the design of the feedback controller, thanks to its robustness properties, in particular against matched disturbances. Early researches on the adoption of SMC in ABS date back to the early 90's. In [8], for instance, an adaptive sliding-mode vehicle traction control strategy is proposed, whereas in [9] the optimum friction is reached without a-priori knowledge of the friction curve.

Most of the research on wheel-slip control with SMC techniques has involved First Order Sliding Mode (FOSM) control, with the focus being placed on the observation of necessary signals [10] or with different approaches to chattering reduction [11], [12]. More recently, Higher Order Sliding Mode (HOSM) control techniques have been implemented. In [13], based on a bicycle model, torques on front and rear axles are controlled so that a target wheel-slip value is tracked on each axle.

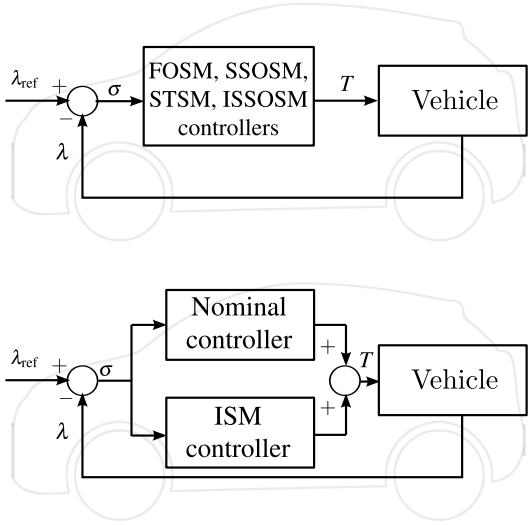

Fig. 1. Sliding Mode slip control schemes

In [14], the so called Suboptimal Second Order Sliding Mode (SSOSM) technique is used for the Traction Control in a motorcycle. In [15] a Super-Twisting Sliding Mode (STSM) control is coupled with linear observers for traction forces, with the focus being on robustness against parameter uncertainties. Evaluation is done through simulation and single-wheel test rig, and shows good results in comparison with Model Predictive Control (MPC).

A sliding mode controller with conditional integrator is tested on a prototype vehicle in [16]: an integral component is added to the sliding variable, so that a PI-like effect is obtained inside a boundary layer. A similar algorithm where a SMC is combined with PI control is presented in [17].

The aim of this paper is to assess the different SMC techniques proposed in recent years to solve the wheel-slip control problem, and compare their performances in different uncertainty conditions (see Figure 1). This work is a preliminary step in determining which SMC technique is more suitable for implementation on a vehicle, with the final goal of successfully run the most suitable algorithms on a

This is the final version of the accepted paper submitted for inclusion in the Proceedings of the American Control Conference, Seattle, WA, May, 2017. Work supported by EU Project ITEAM (project reference: 675999). G. P. Incremoan, E. Regolin, A. Mosca and A. Ferrara are with the Dipartimento di Ingegneria Industriale e dell'Informazione, University of Pavia, via Ferrata 5, 27100 Pavia, Italy (e-mail: gp.incremona@gmail.com, enrico.regolin@unipv.it, alessio.mosca01@universitadipavia.it, a.ferrara@unipv.it)

real multi-actuated electric vehicle.

II. Vehicle Model and Problem Formulation

The model of the vehicle considered in this paper is a nonlinear single-track model [3], i.e., the longitudinal dynamics of the vehicle is given by the following equations

$$\begin{cases} m\dot{v} = 2\left[F_{x,\mathrm{f}}(\lambda_\mathrm{f}) + F_{x,\mathrm{r}}(\lambda_\mathrm{r})\right] - F_{\mathrm{loss}_i}(v) & \text{(1a)} \\ J_\mathrm{f}\dot{\omega}_\mathrm{f} = T_\mathrm{f} - r_\mathrm{f}F_{x,\mathrm{f}}(\lambda_\mathrm{f}) & \text{(1b)} \\ J_\mathrm{r}\dot{\omega}_\mathrm{r} = T_\mathrm{r} - r_\mathrm{r}F_{x,\mathrm{r}}(\lambda_\mathrm{r}) & \text{(1c)} \\ F_\mathrm{loss}(v) = F_\mathrm{air}(v) + F_\mathrm{roll} & \text{(1d)} \\ \qquad\qquad = c_x v^2\,\mathrm{sgn}(v) + f_\mathrm{roll}mg & \\ F_{x,\mathrm{f}} = \mu_{\mathrm{p,f}}(\lambda_\mathrm{f})F_{z,\mathrm{f}} & \text{(1e)} \\ F_{x,\mathrm{r}} = \mu_{\mathrm{p,r}}(\lambda_\mathrm{r})F_{z,\mathrm{r}} & \text{(1f)} \\ F_{z,\mathrm{f}} = \dfrac{l_\mathrm{r}mg - l_\mathrm{h}m\dot{v}}{2(l_\mathrm{f}+l_\mathrm{r})} & \text{(1g)} \\ F_{z,\mathrm{r}} = \dfrac{l_\mathrm{f}mg + l_\mathrm{h}m\dot{v}}{2(l_\mathrm{f}+l_\mathrm{r})} & \text{(1h)} \end{cases}$$

where $\omega = [\omega_\mathrm{f},\ \omega_\mathrm{r}]^T$ is the wheel angular velocity vector, $T = [T_\mathrm{f},\ T_\mathrm{r}]^T$ is the input torque on the wheels, F_x is the traction force on a wheel, F_z is the normal force on a wheel, F_air is the air drag, and F_roll is the rolling resistance. Note that the subscripts "f" and "r" stand for "front" and "rear", respectively. Moreover, m is the mass, c_x is the longitudinal wind drag coefficient, f_roll is the rolling resistance coefficient, J is the wheel moment of inertia, $\mu_{\mathrm{p},\nu} \in [0,\ 1]$ is the tire-road friction coefficient, $r = [r_\mathrm{f},\ r_\mathrm{r}]^T$ is the wheels radius, l_f is the distance from the front axle to the center of gravity (CoG), l_r is the distance from the CoG to the rear axle, and l_h is the vertical distance to the CoG.

A. Wheel Slip Dynamics

System (1) is expressed as a function of the slip ratio $\lambda = [\lambda_\mathrm{f},\ \lambda_\mathrm{r}]^T$ which is defined as

$$\lambda_\nu = \frac{\omega_\nu r_\nu - v_x}{\max(\omega_\nu r_\nu, v_x)},\ \nu = \{\mathrm{f},\mathrm{r}\} \tag{2}$$

More specifically, in case of acceleration, i.e., $\omega_\nu r_\nu > v_x$ and $\omega_\nu \neq 0$, one has

$$\lambda_{\mathrm{a},\nu} = \frac{\omega_\nu r_\nu - v_x}{(\omega_\nu r_\nu)} \tag{3}$$

with wheel slip dynamics given by

$$\dot{\lambda}_{\mathrm{a},\nu} = -\frac{\dot{v}_x}{r_\nu\omega_\nu} - \frac{v_x F_{x,\nu}}{J_\nu\omega_\nu^2} + \frac{v_x}{J_\nu r_\nu\omega_\nu^2}T_\nu \tag{4}$$

Analogously, in case of breaking, i.e., $\omega_\nu r_\nu < v_x$ and $v_x \neq 0$, one has

$$\lambda_{\mathrm{b},\nu} = \frac{\omega_\nu r_\nu - v_x}{v_x} \tag{5}$$

with dynamics given by

$$\dot{\lambda}_{\mathrm{b},\nu} = -\frac{r_\nu\omega_\nu\dot{v}_x}{v_x^2} - \frac{r_\nu^2 F_{x,\nu}}{J_\nu v_x} + \frac{v_x}{J_\nu r_\nu\omega_\nu^2}T_\nu \tag{6}$$

Note that the subscripts "a" and "b" stand for "acceleration" and "breaking", respectively. In this paper roll and yaw moments, lateral and vertical motions, brake, throttle, steering actuators and manifold dynamics are neglected. As for the c_x coefficient, in order to verify the effectiveness of the proposed control schemes in presence of uncertainties, this can vary over time. Also the mass of the vehicle and the tire-road friction coefficient are time-varying and represent the unmatched uncertainties affecting the system.

Moreover, relying on the control variables T_f and T_r, the total available braking torque T_brake, and the engine torque exerted on the driving shaft T_shaft can be calculated. They are regarded as reference signals for the throttle angle controller and for the brake controller, respectively [3].

B. Problem Statement

On the basis of the vehicle model (1)-(6) the following control problem can be stated: *Given a slip reference value λ_ref, find a bounded control law such that the slip error is steered to zero in a finite time in spite of matched and unmatched uncertainties affecting the system, as well as transmission delays in both the feedback and actuation path.*

III. Some Preliminaries on the Application of Sliding Mode Control to the Slip Control Problem

In order to apply the sliding mode control methodology to solve the considered control problem, the so-called sliding variable needs to be defined. In this case we select $\sigma = [\sigma_\mathrm{f},\ \sigma_\mathrm{r}]^T$ as

$$\sigma_\nu = e_{\lambda_\nu} = \lambda_{\mathrm{ref},\nu} - \lambda_\nu, \quad \nu = \{\mathrm{f},\mathrm{r}\} \tag{7}$$

where $\lambda_{\mathrm{ref},\nu}$ is the desired value of the slip ratio. Let ρ be the relative degree of the system, i.e., the minimum order of the time derivative of the sliding variable, $\sigma_\nu^{(\rho)}$, in which the control input T_ν explicitly appears. Now, compute the first and the second time derivative of the sliding variable, so that by posing $\xi_{1,\nu} = \sigma_\nu$ and $\xi_{2,\nu} = \dot{\sigma}_\nu$, the so-called auxiliary system can be written as

$$\begin{cases} \dot{\xi}_{1,\nu}(t) &= \xi_{2,\nu}(t) \\ \dot{\xi}_{2,\nu}(t) &= f_{\pi,\nu}(t) + g_{\pi,\nu}(t)w(t),\ \pi = \{\mathrm{a},\mathrm{b}\},\ \nu = \{\mathrm{f},\mathrm{r}\} \end{cases} \tag{8}$$

where $w(t) = \dot{T}_\nu$ is the auxiliary control variable, while the function $f_{\pi,\nu}(\cdot)$ and $g_{\pi,\nu}(\cdot)$ are

$$\begin{aligned} f_{\mathrm{a},\nu}(t) = \quad & \ddot{\lambda}_{\mathrm{ref},\nu} + \tfrac{\ddot{v}_x}{r_\nu\omega_\nu} - \tfrac{\dot{v}_x\dot{\omega}_\nu}{r_\nu\omega_\nu^2} + \tfrac{\dot{v}_x F_{x,\nu}}{J_\nu\omega_\nu^3} + \tfrac{\dot{v}_x\dot{F}_{x,\nu}}{J_\nu\omega_\nu^2} + \\ & - \tfrac{2v_x F_{x,\nu}\dot{\omega}_\nu}{J_\nu^2\omega_\nu^3} - \tfrac{v_x T_\nu\dot{\omega}_\nu}{J_\nu^2 r_\nu\omega_\nu^3} - \tfrac{\dot{v}_x T_\nu}{J_\nu^2 r_\nu\omega_\nu^2} \\ f_{\mathrm{b},\nu}(t) = \quad & \ddot{\lambda}_{\mathrm{ref},\nu} + \tfrac{r_\nu\dot{\omega}_\nu}{v_x} + \tfrac{r_\nu\omega_\nu\dot{v}_x}{v_x^2} + \tfrac{r_\nu^2\dot{F}_{x,\nu}}{J_\nu v_x} - \tfrac{r_\nu^2 F_{x,\nu}\dot{v}_x}{J_\nu v_x^2} + \\ & - \tfrac{2r_\nu\omega_\nu\dot{v}_x}{v_x^2} - \tfrac{v_x T_\nu\dot{\omega}_\nu}{J_\nu^2 r_\nu\omega_\nu^3} - \tfrac{\dot{v}_x T_\nu}{J_\nu^2 r_\nu\omega_\nu^2} \\ g_{\pi,\nu}(t) = \quad & -\tfrac{v_x}{J_\nu r_\nu\omega_\nu^2} \end{aligned} \tag{9}$$

Since velocities are assumed to be always positive and physical limits exist such as the limit characteristic curves of the torques which the engine can transfer to the wheels,

it is assumed that functions $f_{\pi,v}(\cdot)$ and $g_{\pi,v}(\cdot)$ are bounded, with, in particular

$$|f_{\pi,v}(t)| \leq F \tag{10}$$

$$-G_{\max} \leq g_{\pi,v}(t) \leq -G_{\min} < 0 \tag{11}$$

$$|w(t)| \leq W \tag{12}$$

where F, $G_{\min}$, $G_{\max}$ and W are positive constants, which in practical cases can be estimated and are therefore assumed known.

IV. The Considered Sliding Mode Control Strategies

The proposed slip control schemes are illustrated in Figure 1. In this paper different sliding mode control strategies are discussed. More specifically, in the following subsections a FOSM control [18], a SSOSM control [19], a STSM control [20], an Integral Sliding Mode (ISM) control [21] and the recently published Integral SSOSM (ISSOSM) control algorithm [22] are considered. Consider now the first control scheme of Figure 1.

A. FOSM Control

The first strategy discussed in this paper is the classical FOSM control [18]. Given the choice of the sliding variable (7), the relative degree is $\rho = 1$ so that a FOSM naturally applies. The control law in this case is

$$T_v(t) = -U_{v,\max} \operatorname{sgn}(\sigma_v(t)) \tag{13}$$

where the control parameter $U_{v,\max}$ is a positive constant chosen so as to enforce a sliding mode [18]. The main difficulty with applying of this approach to solve the slip control problem is the discontinuity of the control variable which can cause chattering phenomenon [23] which is hardly acceptable.

B. SSOSM Control

SSOSM control is a particular case of HOSM control (see, for instance, [24] and [25] for other second order sliding mode algorithms). Given the auxiliary system (8), in which the relative degree is artificially increased by introducing the auxiliary control variable w, the control law can be expressed as

$$T_v(t) = -\int_{t_0}^{t} \alpha_v W_{v,\max} \operatorname{sgn}\left(\xi_{1,v}(\zeta) - \tfrac{1}{2}\xi_{\max}\right) d\zeta \tag{14}$$

where $\xi_{\max}$ is the local minimum or maximum of the sliding variable, while the control parameters $\alpha_v = \alpha_v^*$ and $W_{v,\max}$ are chosen such that

$$W_{v,\max} > \max\left(\frac{F}{\alpha_v^* G_{\min}}; \frac{4F}{3G_{\min} - \alpha_v^* G_{\max}}\right) \tag{15}$$

$$\alpha_v^* \in (0,1] \cap \left(0, \frac{3G_{\min}}{G_{\max}}\right) \tag{16}$$

Note that the SSOSM algorithm requires the control $w(t) = \dot{T}_v(t)$ to be discontinuous. Yet, the control actually fed into the plant is continuous, which is highly appreciable in case of mechanical plants. Moreover, in [19] it has been proved that, under constraints (15), the convergence of the auxiliary system trajectory to the origin takes place in a finite time. More specifically, the control law (14) implies a contraction property of the extremal values of the sliding variable so that the slip error and its first time derivative are steered to zero in a finite time. Moreover, an important advantage of the SSOSM control is that the knowledge of the first time derivative of the sliding variable is not required, but only the computation of its extremal values, for instance through the methods described in [19].

C. STSM Control

STSM control is another particular case of second order sliding mode control in which, similarly to the SSOSM algorithm, the knowledge of the first time derivative of the sliding variable is not required [20]. The STSM control law can be expressed as

$$\begin{aligned} T_v(t) &= v_v(t) - W_{v,\max}\sqrt{|\xi_{1,v}(t)|}\operatorname{sgn}\left(\xi_{1,v}(t)\right) \\ \dot{v}_v(t) &= -V_{v,\max}\operatorname{sgn}\left(\xi_{1,v}(t)\right) \end{aligned} \tag{17}$$

where $W_{v,\max}$ and $V_{v,\max}$ are suitably chosen in order to ensure the sliding mode [20].

D. ISSOSM Control

In this subsection, the recently introduced ISSOSM control methodology is recalled [22]. This represents an extension of the SSOSM control algorithm with improved robustness properties against the uncertainties affecting the system. The idea is to reduce to a minimum the so-called reaching phase [18], during which the controlled system is not insensitive to the disturbances. Consider the auxiliary system (8) and define a *transient function* as

$$\begin{cases} \varphi_v(t) = (t-t_{\mathrm{r}})^2(c_0 + c_1(t-t_0)), & \forall t,\ t_0 \leq t \leq t_{\mathrm{r}} \\ \varphi_v(t) = 0, & \forall t > t_{\mathrm{r}} \end{cases} \tag{18}$$

where c_0 and c_1 are

$$c_0 = \sigma_v(t_0)T^{-2} \tag{19}$$

$$c_1 = \dot{\sigma}_v(t_0)T^{-2} + 2\sigma_v(t_0)T^{-3} \tag{20}$$

while $T = t_{\mathrm{r}} - t_0$ is the so-called "prescribed time", which allows one to steer the sliding variable σ_v to zero at the time t_{r}. Note that, from (19) and (20), the transient function is realized such that the initial conditions are

$$\sigma_v(t_0) = \varphi_v(t_0) \tag{21}$$

$$\dot{\sigma}_v(t_0) = \dot{\varphi}_v(t_0) \tag{22}$$

Then, the auxiliary sliding manifold is defined as

$$\Sigma_v(t) = \sigma_v(t) - \varphi_v(t) = 0 \tag{23}$$

where Σ_v is an auxiliary sliding variable such that $\xi_{1\,v} = \Sigma_v$ and $\xi_{2\,v} = \dot{\Sigma}_v$, while the control law is of the same form of (14) with constraints as in (15) and (16). The finite time convergence of the sliding variable in front of matched uncertainties can be proved relying on the results presented in [22].

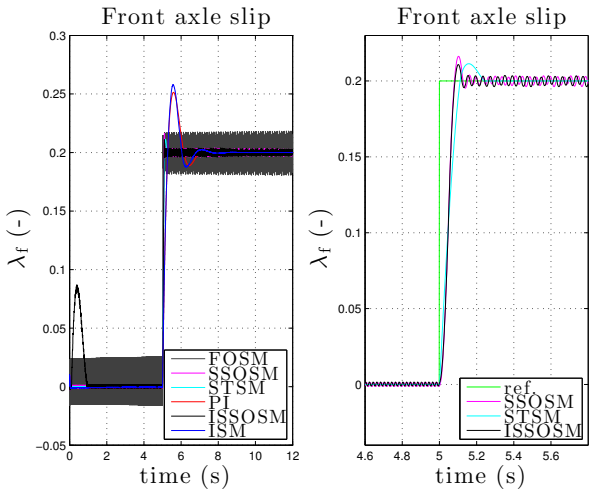

Fig. 2. Step response of the controllers when disturbances are not present (left), and detail of the step response of the SSOSM, STSM and ISSOSM algorithms (right)

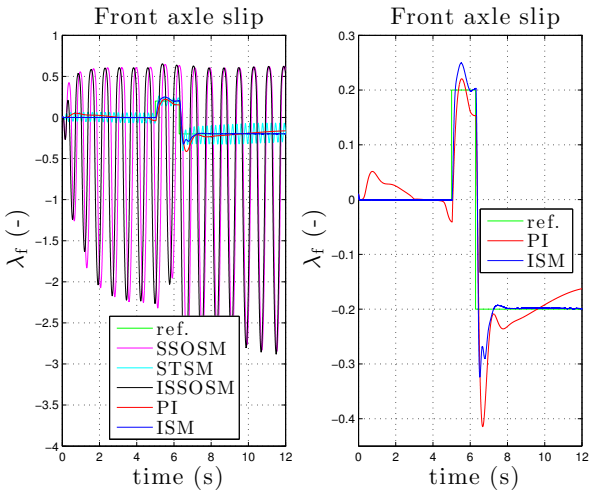

Fig. 3. Step response of the controllers when all the disturbances are present (left), and detail with only PI and ISM controllers (right)

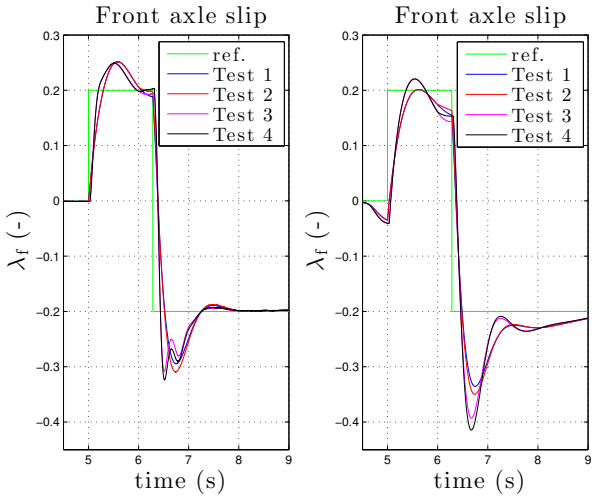

Fig. 4. Difference in the controller performance in presence of different disturbances combinations when ISM (left) and PI (right) controllers are used

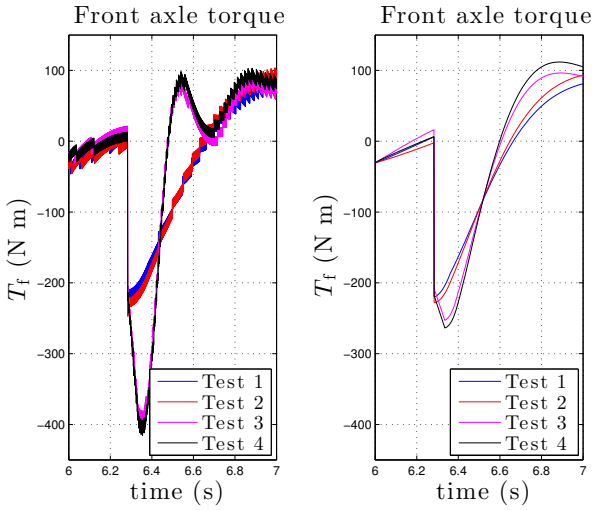

Fig. 5. Detail of the control signals corresponding to controllers in Figure 4. Note that in the tests with delay, the increase of the control action is considerably stronger with the ISM controller

E. ISM Control

Now, consider the second control scheme in Figure 1. ISM method enables to generate an ideal sliding mode of the controlled system starting from the initial time instant t_0 [21]. The ISM control variable is split into two parts

$$T_v(t) = T_{v,0}(t) + T_{v,1}(t) \tag{24}$$

where $T_{v,0}(t)$ is generated by any suitably designed high level controller, for instance a PI controller as in this paper, and $T_{v,1}(t)$ is a discontinuous control action designed to compensate the uncertainties affecting the system. The so-called integral sliding manifold is defined as in (23), where the integral term φ_v is

$$\varphi_v(t) = \sigma_v(t_0) + \int_{t_0}^{t} \frac{\partial \sigma_v}{\partial e_{\lambda_v}} \dot{e}_{\lambda_v}(\zeta) d\zeta \tag{25}$$

with the initial condition $\varphi_v(t_0) = \sigma_v(t_0)$. The ISM control law is then defined as

$$T_{v,1}(t) = -U_{v,\max} \operatorname{sgn}(\Sigma_v(t)) \tag{26}$$

with $U_{v,\max} > 0$ to enforce the sliding mode. By virtue of the choice of $\varphi_v(t)$ and $\varphi_v(t_0)$, it is apparent that the controlled system is in sliding mode on the manifold $\Sigma_v(t) = 0$ since the initial time instant. Moreover, under suitable assumptions on the auxiliary sliding variable, it is possible to show that the unmatched uncertainties are not amplified [21].

V. Simulations

In this section the sliding mode controllers are evaluated in a step response test, where the wheel-slip is regulated to a fixed value. A PI controller is also used in the same test for the sake of comparison. It is assumed that the maximum

traction/braking force is obtained for $\lambda_{\text{ref},\nu} = \pm 0.2$ (the sign corresponds to the sign of the driver's torque demand, which is considered a matched disturbance in this work).

A. Test Setup

The presented controllers are evaluated in 4 different conditions:

1) matched uncertainties;
2) matched and parameters uncertainties;
3) matched uncertainties and delays;
4) matched, parameters uncertainties and delays.

Matched disturbances are always included, as their rejection is the main advantage of using SMC. They consist of sinusoidal torques which induce an acceleration or a braking phase on each axle, depending on the torque sign. With the purpose of showing the controllers robustness against unmatched disturbances, in Tests 2 and 4 time varying parameter uncertainties on vehicle mass, drag coefficient and road friction coefficient are included. Results on front and rear axles are almost identical, as the only parametric differences affecting the respective dynamics are the geometric ones introduced in equations (1g) and (1h). For this reason, in this section only results on the front axle are shown.

In Tests 3 and 4 delays are introduced on the acquired signals used for control (20 ms) and on the actuation (50 ms). Modeling of the actual delays found on a vehicle would require a far deeper analysis, including studies on sensors, CAN bus and actuators dynamics: nevertheless, assessing the response of the proposed controllers in the presence of a generic delay helps evaluating which SMC is more suitable to be implemented in a real test environment.

Please note that in the ISM design a nominal controller is required to be included, whereas it is not necessary in the other SMCs. The nominal control is the same PI algorithm used in the standalone experiment. All controllers parameters have been tuned in order to obtain an adequate response for each algorithm.

B. Results

In Figure 2 the step response of all considered controllers is shown, when no disturbances or delays are applied. It can be observed that FOSM and ISSOSM have strong oscillations, which vanish too slowly at steady state, or do not vanish at all in case of FOSM. The PI and ISM controllers show the highest overshoot and longest settling time, but nevertheless they converge to the reference value at steady state. It can be observed more in detail in the second graph of Figure 2, that the STSM algorithm has slightly higher settling time and lower steady state oscillations.

In Figure 3 the same controllers are evaluated against disturbances and delays, except for FOSM and ISSOSM, whose behavior was found to be unsatisfactory, even with no disturbances. SOSM and ISSOSM, although not unstable, show oscillations induced by the delays which cannot be accepted: the high gain in the SMC reduces the robustness to delays, the same way increasing the gain in a linear system reduces the phase margin. The STSM algorithm shows a better response, yet the chattering induced by the delay exceeds the 50% of the target wheel-slip value. The best performance is the one guaranteed by the PI and ISM controllers, which are shown in detail in the second graph of Figure 3. While the conventional controller, even with a strong integral action, struggles to bring the steady state error to zero, the ISM neutralizes the effect of the matched disturbances, thanks to its discontinuous control action, without increasing the overall system bandwidth. The ISM shows a better step response than the PI both in the transient and at steady state, with faster response, reduced overshoot and steady state convergence.

TABLE I

RMS ERROR $e_{\text{RMS},\nu}$, $\nu = \{\text{f},\text{r}\}$

Test	FOSM	SSOSM	STSM	PI	ISSOSM	ISM
1	0.0217	0.0364	0.0320	0.0534	0.0384	0.0456
	0.0215	0.0359	0.0319	0.0540	0.0380	0.0464
2	0.0216	0.0365	0.0323	0.0553	0.0383	0.0477
	0.0221	0.0357	0.0322	0.0554	0.0382	0.0478
3	0.3562	1.3307	0.0740	0.0654	1.3496	0.0535
	0.3584	1.4793	0.0750	0.0665	1.4089	0.0544
4	0.3506	1.3731	0.0716	0.0680	1.3960	0.0554
	0.3520	1.4131	0.0726	0.0683	1.3748	0.0557

TABLE II

RMS VALUE OF CONTROL SIGNAL $E_{\text{c},\nu}$, $\nu = \{\text{f},\text{r}\}$

Test	FOSM	SSOSM	STSM	PI	ISSOSM	ISM
1	1300	146.1	134.0	133.9	146.0	133.4
	1300	150.4	138.5	138.2	150.3	137.1
2	1300	150.8	138.4	138.4	150.8	138.0
	1300	153.4	141.0	140.9	153.5	140.0
3	1300	1070.9	208.5	136.2	1073.4	138.4
	1300	1123.4	211.8	140.7	1092.0	142.4
4	1300	1088.8	209.3	141.0	1095.1	143.1
	1300	1112.6	211.2	143.6	1094.5	145.1

In Figure 4 the effect of the different disturbances and delays when the PI and ISM controllers are applied is shown. It can be seen that on both controllers parameter uncertainties have a minor impact compared to the matched uncertainties, as it is confirmed by the Root Mean Square (RMS) error values in Table I (e_{RMS}). Moreover, Table II reports the values of the control effort, E_{c}, for all controllers.

The delay, on the other hand, has a significant impact: in the PI controlled system it increases the overshoot, while in the ISM case the delay makes the response even faster, with no overshoot increase. This effect is due to the increased control action (see Figure 5) induced by the nonlinear control, which is up to the 68% of the original value, compared to the increment of only the 15% with the conventional controller.

C. Controllers Evaluation

The performance indices reported in Tables I and II help us assessing the different controllers considered in this paper.

The FOSM control is the most aggressive solution: it ensures a good e_{RMS} in all the considered conditions, while at the same time it has a control signal RMS E_{c} which is larger than those of all other controllers by one order of magnitude.

This fact makes such a controller a non feasible solution, once the actuators limitations and dynamics are taken into account.

As verified in simulation, when delays are not present, the SMC controllers are able to reject the matched uncertainties affecting the system and they result sufficiently insensitive even to parameters variations (unmatched disturbances). More specifically, by construction, the ISSOSM and the ISM controllers are robust from the initial time instant. The second order algorithms have the smallest e_{RMS} of the remaining controllers, when considering tests with no delay. Their respective control signal RMS values E_{c} are comparable to the ones of the PI and ISM controllers.

When the delays are introduced, the SSOSM and the ISSOSM are no more acceptable. In fact, both the algorithms are based on the presence of a peak detector to find the extremal values of the sliding variable. This device is implemented in a discrete time way by comparing the signals in subsequent time instants. This implies that the extremal values in presence of delays are corrupted, causing an oscillatory behavior which can be critical for the considered system. The STSM does not include a peak detection, so that the deterioration of the performance is not as sharp.

The best performance in the presence of delays is guaranteed by the ISM controller. In this case, while the discontinuous component is able to reject the matched uncertainties affecting the system, the nominal component (see Figure 1, second scheme) is robust enough in front of delays, since it has the effect of reducing the bandwidth of the equivalent controlled system, thus increasing its phase margin. On top of this expected behavior, the discontinuous action appears to positively impact the system response in the presence of delays, which is particularly evident in Figure 5.

VI. Conclusions

In this paper, the assessment of sliding mode control algorithms for wheel slip control of road vehicles has been presented. In particular, this work focuses on the impact of uncertainties and delays on the different controllers. While the first order sliding mode algorithm has comparable results with and without delay, due to its aggressive nature it is not suited for being utilized in this context. The second order sliding mode algorithms are characterized by excellent performances in presence of disturbances, which deteriorate in presence of delays. The proposed ISM controller offers the most encouraging results, which allows us to conclude, at the best of our knowledge, that this kind of controller can be a good candidate for application to a real vehicle.

References

[1] V. Ivanov, D. Savitski, and B. Shyrokau, "A survey of traction control and antilock braking systems of full electric vehicles with individually controlled electric motors," *IEEE Transactions on Vehicular Technology*, vol. 64, no. 9, pp. 3878–3896, Sep. 2015.

[2] H. Pacejka and E. Bakker, "The magic formula tyre model," *Vehicle Systems Dynamics*, vol. 21, pp. 1–18, 1993.

[3] G. Genta, *Motor Vehicle Dynamics - Modeling and Simulation*. Singapore: World Scientific, 1993.

[4] H. Imine, L. Fridman, H. Shraim, and M. Djemai, *Sliding Mode Based Analysis and Identification of Vehicle Dynamics*, ser. Lecture Notes in Control and Information Sciences. Springer-Verlag Berlin Heidelberg, 2011, vol. 414.

[5] M. Tanelli, A. Ferrara, and P. Giani, in *Proc. IEEE International Conference on Control Applications*, Dubrovnik, Croatia, Oct.

[6] M. Reichhartinger, S. K. Spurgeon, and M. Weyrer, "Design of an unknown input observer to enhance driver experience of electric power steering systems," in *European Control Conference*, Aalborg, Denmark, Jul. 2016.

[7] R. Tafner, M. Horn, and A. Ferrara, "Experimental evaluation of nonlinear unknown input observers applied to an eps system," in *Proc. American Control Conference*, Boston, MA, Jul. 2016, pp. 2409–2414.

[8] H. S. Tan and M. Tomizuka, "An adaptive sliding mode vehicle traction controller design," in *Proc. American Control Conference*, San Diego, CA, May 1990, pp. 1856–1862.

[9] S. Drakunov, U. Ozguner, P. Dix, and B. Ashrafi, "Abs control using optimum search via sliding modes," *IEEE Transactions on Control Systems Technology*, vol. 3, no. 1, pp. 79–85, Mar. 1995.

[10] C. Unsal and P. Kachroo, "Sliding mode measurement feedback control for antilock braking systems," *IEEE Transactions on Control Systems Technology*, vol. 7, no. 2, pp. 271–281, Mar. 1999.

[11] J. J. Moskwa and J. K. Hedrick, "Sliding mode control of automotive engines," in *Proc. American Control Conference*, Pittsburgh, PA, Jun. 1989, pp. 1040–1045.

[12] C.-M. Lin and C. F. Hsu, "Neural-network hybrid control for antilock braking systems," *IEEE Transactions on Neural Networks*, vol. 14, no. 2, pp. 351–359, Mar. 2003.

[13] M. Amodeo, A. Ferrara, R. Terzaghi, and C. Vecchio, "Wheel slip control via second-order sliding-mode generation," *IEEE Transactions on Intelligent Transportation Systems*, vol. 11, no. 1, pp. 122–131, Mar. 2010.

[14] M. Tanelli, C. Vecchio, M. Corno, A. Ferrara, and S. M. Savaresi, "Traction control for ride-by-wire sport motorcycles: A second-order sliding mode approach," *IEEE Transactions on Industrial Electronics*, vol. 56, no. 9, pp. 3347–3356, Sep. 2009.

[15] S. Kuntanapreeda, "Super-twisting sliding-mode traction control of vehicles with tractive force observer," *Control Engineering Practice*, vol. 38, pp. 26–36, Feb. 2015.

[16] R. de Castro, R. E. Araújo, and D. Freitas, "Wheel slip control of evs based on sliding mode technique with conditional integrators," *IEEE Transactions on Industrial Electronics*, vol. 60, no. 8, pp. 3256–3271, Aug. 2013.

[17] Y. Wang and Z. Sun, "Dynamic analysis and multivariable transient control of the power-split hybrid powertrain," *IEEE/ASME Transactions on Mechatronics*, vol. 20, no. 6, pp. 3085–3097, Dec 2015.

[18] V. I. Utkin, *Sliding Modes in Optimization and Control Problems*. New York: Springer Verlag, 1992.

[19] G. Bartolini, A. Ferrara, and E. Usai, "Chattering avoidance by second-order sliding mode control," *IEEE Transactions on Automatic Control*, vol. 43, no. 2, pp. 241–246, Feb. 1998.

[20] A. Levant, "Higher-order sliding modes, differentiation and output-feedback control," *International Journal of Control*, vol. 76, no. 9–10, pp. 924–941, Jan. 2003.

[21] V. I. Utkin and J. Shi, "Integral sliding mode in systems operating under uncertainty conditions," in *Proc. 35th IEEE Conference on Decision and Control*, vol. 4, Kobe, Japan, Dec. 1996, pp. 4591–4596.

[22] A. Ferrara and G. P. Incremona, "Design of an integral suboptimal second order sliding mode controller for the robust motion control of robot manipulators," *IEEE Transactions on Control Systems Technology*, vol. 23, no. 6, pp. 2316–2325, May 2015.

[23] A. Levant, "Chattering analysis," *IEEE Trans. Automat. Control*, vol. 55, no. 6, pp. 1380 –1389, Jun. 2010.

[24] G. Bartolini, A. Ferrara, A. Levant, and E. Usai, "On second order sliding mode controllers," in *Variable Structure Systems, Sliding Mode and Nonlinear Control*, ser. Lecture Notes in Control and Information, K. D. Young and Ü. Özgüner, Eds. London, UK: Springer-Verlag, 1999, pp. 329–350.

[25] F. Dinuzzo and A. Ferrara, "Higher order sliding mode controllers with optimal reaching," *IEEE Transactions on Automatic Control*, vol. 54, no. 9, pp. 2126 –2136, Sep. 2009.